

Investigation of negative-parity states in ^{16}C via deuteron inelastic scattering*

Z. W. Tan(谭智威)¹ J. L. Lou(楼建玲)^{1†} Y. L. Ye(叶沿林)¹ Y. Liu(刘洋)^{1,8} D. Y. Pang(庞丹阳)²
 C. X. Yuan(袁岑溪)³ J. G. Li(李健国)⁴ W. Liu(刘威)¹ Y. Jiang(蒋颖)¹ B. Yang(杨彪)¹ L. C. Tao(陶龙春)¹
 K. Ma(马凯)¹ Z. H. Li(李智焕)¹ Q. T. Li(李奇特)¹ X. F. Yang(杨晓菲)¹ J. Y. Xu(许金艳)¹ H. Z. Yu(余瀚舟)¹
 J. X. Han(韩家兴)¹ S. W. Bai(白世伟)¹ S. W. Huang(黄思维)¹ G. Li(李根)¹ H. Y. Wu(吴鸿毅)¹
 H. L. Zang(臧洪亮)¹ J. Feng(冯俊)¹ J. S. Wang(王建松)⁴ Y. Y. Yang(杨彦云)⁴ P. Ma(马朋)⁴ Q. Hu(胡强)⁴
 Z. Bai(白真)⁴ Z. H. Gao(高志浩)⁴ F. F. Duan(段芳芳)⁴ L. Y. Hu(胡力元)⁵ J. H. Tan(谭金昊)⁵
 S. Q. Sun(孙诗奇)⁵ Y. S. Song(宋玉收)⁵ H. J. Ong(王惠仁)^{4,6} D. T. Tran^{6,7}
 H. Y. Zhu(朱宏渝)¹ B. L. Xia(夏博龙)¹

¹School of Physics and State Key Laboratory of Nuclear Physics and Technology, Peking University, Beijing 100871, China

²School of Physics, Beijing Key Laboratory of Advanced Nuclear Materials and Physics, Beihang University, Beijing 100191, China

³Sino-French Institute of Nuclear Engineering and Technology, Sun Yat-Sen University, Zhuhai 519082, China

⁴Institute of Modern Physics, Chinese Academy of Sciences, Lanzhou 730000, China

⁵Fundamental Science on Nuclear Safety and Simulation Technology Laboratory, Harbin Engineering University, Harbin 150001, China

⁶Research Center for Nuclear Physics, Osaka university, Osaka 567-0047, Japan

⁷Institute of Physics, Vietnam Academy of Science and Technology, Hanoi 10000, Vietnam

⁸Institute of Materials, China Academy of Engineering Physics, Mianyang 621907, China

Abstract: Two low-lying unbound states in ^{16}C are investigated by deuteron inelastic scattering in inverse kinematics. Besides the 2^- state at 5.45 MeV previously measured in a $1n$ knockout reaction, a new resonant state at 6.89 MeV is observed for the first time. The inelastic scattering angular distributions of these two states are well reproduced by the distorted-wave Born approximation (DWBA) calculation with an $l = 1$ excitation. In addition, the spin-parities of the unbound states are discussed and tentatively assigned based on shell model calculations using the modified YSOX interaction.

Keywords: negative-parity states, inelastic scattering, ^{16}C

DOI: 10.1088/1674-1137/ac488b

I. INTRODUCTION

One of the most important questions in the study of unstable neutron-rich nuclei is the evolution of shell structures, such as a rapid change of the $1s_{1/2}$ orbit relative to the $0d_{5/2}$ and $0p_{1/2}$ orbits in the nuclei around $N = 8$ [1, 2]. This variation can lead to the disappearance of conventional magic number $N = 8$ and the appearance of new magic number $N = 14$ or $N = 16$. Our experimental results obtained from the single-nucleon transfer reactions of ^{11}Be on proton and deuteron targets imply the breakdown of the magic number $N = 8$ and the strong intrusion of the sd -shell in ^{11}Be and ^{12}Be [3-9]. As another well-known example, a systematic comparison of the energies of the 2^+ states in neutron-rich oxygen and carbon isotopes and the study of the evolution of single-particle

levels in ^{17}C suggests that the $N = 14$ sub-shell is absent for $Z = 6$ [10, 11]. In ^{13}C , ^{15}C , and ^{17}C , the excitation energies of the $5/2^+$ states are higher than the $1/2^+$ states [12], demonstrating the inversion of $1s_{1/2}$ and $0d_{5/2}$ orbitals in comparison with the conventional shell model.

For the neutron-rich nucleus ^{16}C , its bound excited states and high-lying unbound states have been intensively studied by various experiments; see Refs. [13-16] and references therein. However, apart from one $2n$ transfer reaction [17, 18] and one knockout experiment of ^{17}C on a proton target [19], the experimental studies of low-lying unbound states at $E_x = 5-10$ MeV, which are important to well understand the shell gap between sd - and p -shell as well as the ordering of s - and d -shells [20], are scarce. One resonant state at $E_x = 6.11$ MeV was firstly observed in the $^{14}\text{C}(t, p)^{16}\text{C}$ reaction [17, 18, 21]. The lar-

Received 28 December 2021; Accepted 7 January 2022; Published online 9 March 2022

* Supported by the National Key R & D Program of China (2018YFA0404403), the National Natural Science Foundation of China (11775004, U1867214, 11875074, 11961141003), the funding from the State Key Laboratory of Nuclear Physics and Technology, Peking University (NPT2021ZZ01), and the funding from Heavy Ion Research Facility in Lanzhou (HIR2021PY002)

† E-mail: jllou@pku.edu.cn, Corresponding author

©2022 Chinese Physical Society and the Institute of High Energy Physics of the Chinese Academy of Sciences and the Institute of Modern Physics of the Chinese Academy of Sciences and IOP Publishing Ltd

ger $2n$ transfer cross sections for this state suggested that its spin-parity was either of 2^+ , 3^- , or 4^+ [17, 18]. Three unbound states at $E_x = 5.45, 6.11, 6.28$ MeV in ^{16}C were observed by Satou *et al* in a $1n$ knockout reaction [19]. The 5.45 and 6.28 MeV states decay predominately via $1n$ to the first excited state of ^{15}C ($5/2^+$, d -wave), while the 6.11 MeV state decays to the ground state (g.s.) of ^{15}C ($1/2^+$, s -wave). The spin-parity of 2^- was assigned to the 5.45 MeV state because both the excitation energy and the cross section were consistent with theoretical calculations. The negative-parity assignment to this state was further confirmed by the fact that its parallel momentum angular distribution agreed well with a p -wave neutron

knockout from ^{17}C [19]. For the 6.11 MeV state, comparing with theoretical calculations, its excitation energy and the $1n$ knockout cross section preferred the J^π assignment of $2^+/3^-$ rather than 4^+ [19]. Fortune suggested that the 6.11 MeV state was not 3^- , but probably 1^- (0^-) according to the shell model and a simple weak-coupling model [22]. However, Fortune recently concluded that its J^π was 2^+ after investigating its width (32.6(5) keV) from the $^{14}\text{C}(t, p)^{16}\text{C}$ reaction [23]. For the 6.28 MeV state, Satou *et al* suggested that the spin-parities of 1_2^- and 2_2^- were candidates [19], and lately Fortune concluded that its J^π was 2^- [22]. These studies are summarized in Table 1.

Table 1. Summary of spin-parity assignments for the negative-parity states in ^{16}C .

E_x /MeV	$2n$ transfer reaction [17]	$1n$ knockout from ^{17}C [19]	shell model [22]	width [23]	present work
5.45		2^-	2^-		1^- or 2^- *
6.11	$2^+, 3^-, 4^+$	$2^+, 3^-$	$1^-, 0^-$	2^+	
6.28		$1_2^-, 2_2^-$	2^-		
6.89					(1)

*The DWBA calculations support the assignment of 1^- , but the shell model results suggest 2^- .

In this paper, we report on a new measurement of the low-lying unbound states in ^{16}C , which were populated by the deuteron inelastic scattering using a radioactive beam ^{16}C at about 23.5 MeV/nucleon in inverse kinematics. Details of this experiment has been published in Refs. [14-16], and in this paper we only focus on the inelastic scattering of ^{16}C to its unbound states.

II. EXPERIMENT

A ^{16}C secondary beam was produced from a 59.6-MeV/nucleon ^{18}O primary beam impinging on a 4.5-mm-thick ^9Be target. The secondary beam was purified and transmitted by the Radioactive Ion Beam Line in Lanzhou (RIBLL), Institute of Modern Physics (IMP), China. The time-of-flight (TOF) provided by two plastic scintillator detectors and energy losses (ΔE) in a large-surface silicon detector (SSD) were used to identify the secondary beam. The average beam intensity and the purity of ^{16}C were up to about 10^4 particles per second (pps) and 90%, respectively. The beam energy was ~ 23.5 MeV/nucleon.

The experimental setup is given in Refs. [14, 15]. Three parallel-plate avalanche chambers (PPACs) were placed upstream of the physical targets to provide beam tracking information. The resolution of the hit position on the target was ~ 1.0 mm (FWHM, full width at half maximum) in both x and y directions. A 9.53 ± 0.12 mg/cm 2 (CD_2) $_n$ target was used to measure the inelastic scatter-

ing data. A 13.73 ± 0.13 mg/cm 2 carbon target was employed to subtract the background coming from carbon atoms in the (CD_2) $_n$ target. An empty target was also applied to measure random or accidental coincidence events. Several sets of telescopes were installed in a large vacuum chamber to detect and identify charged particles using a standard ΔE - E method. The telescope T_0 and T_2 were placed 156 and 157 mm away from the target to distinguish the carbon isotopes at forward angles and the recoil deuterons emitting to backward angles, respectively. The telescope T_0 installed at around 0° is made up of three 1000- μm -thick double-sided silicon strip detectors (DSSDs), three 1500- μm -thick SSDs, and a layer of 4-cm-thick CsI(Tl) crystals read out by photodiodes. The telescope T_2 , which consists of a 300- μm -thick DSSD, a 1500- μm -thick SSD, and a layer of CsI(Tl) crystals, was placed at $\sim 69^\circ$ relative to the beam direction. Each DSSD with an active area of 63.96 mm \times 63.96 mm is divided into 32 strips on both sides. The angular coverage of the telescopes T_0 and T_2 are $\theta_{\text{lab}}^{T_0} = 0 \sim 12^\circ$ and $\theta_{\text{lab}}^{T_2} = 57^\circ \sim 82^\circ$, respectively. The overall angular resolution of the telescope T_2 was $\sim 0.92^\circ$ (FWHM).

The particle identification (PID) spectra detected by the telescope T_0 in coincidence with the recoil light-charged particles measured by the telescope T_2 are presented in Fig. 2 (a) of Ref. [14]. The carbon isotopes ^{16}C , ^{15}C , and ^{14}C are discriminated clearly. ^{16}C ions were from the elastic or inelastic scattering to the bound states at $E_x = 1.766(2_1^+)$, 3.986, 4.088 and 4.142 MeV in ^{16}C ,

while ^{15}C and ^{14}C particles came from the inelastic scattering to unbound states in ^{16}C which subsequently decay via $1n$ and $2n$, respectively. Note that the second 0^+ state at around $E_x = 3.027$ MeV was hardly populated by the inelastic scattering [14, 24].

With a gate of all carbon isotopes, including ^{16}C , ^{15}C , and ^{14}C , the recoil deuterons detected by the telescope T_2 were used to analyze the elastic and inelastic scattering differential cross sections (DCSs). The energies of the recoil deuterons as a function of their angles in the laboratory frame are displayed in Fig. 1. Most data points agree well with the calculated kinematic curves, indicating that these events are indeed from elastic or inelastic scattering of $^{16}\text{C} + d$. Although the statistics are limited, the 1.766 and 5.45 MeV states are clearly seen. Within the angular range of $60^\circ \sim 66^\circ$ in the laboratory frame, some events are also in line with the blue dotted curve, which stands for the calculated kinematics of a new unbound state at $E_x = 6.89$ MeV.

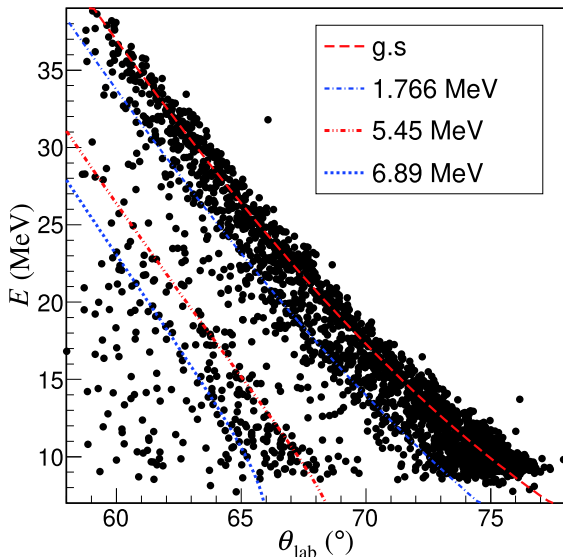


Fig. 1. (color online) Kinematics for the recoil deuterons in coincidence with $^{14,15,16}\text{C}$. The curves are calculated for the elastic scattering and the inelastic scatterings of $^{16}\text{C} + d$ to the 1.766, 5.45, and 6.89 MeV states in ^{16}C .

Figure 2 displays the Q -value spectra deduced from the energies and angles of the recoil deuterons emitted in the angular range between $60^\circ \sim 68^\circ$ in the laboratory frame. The g.s., and the 1.766, ~ 4.0 , 5.45 MeV excited states in ^{16}C are clearly observed. A new resonant state centered at around 6.89 MeV is measured experimentally for the first time. In coincidence with ^{15}C , the Q -value spectrum is illustrated as the grey histograms. Note that the high-energy portion for ^{15}C is prone to be contaminated by the secondary beam ^{16}C , therefore the cut of ^{15}C should be gated not only on the PID spectrum measured by the telescope T0 but also on the two-dimensional (en-

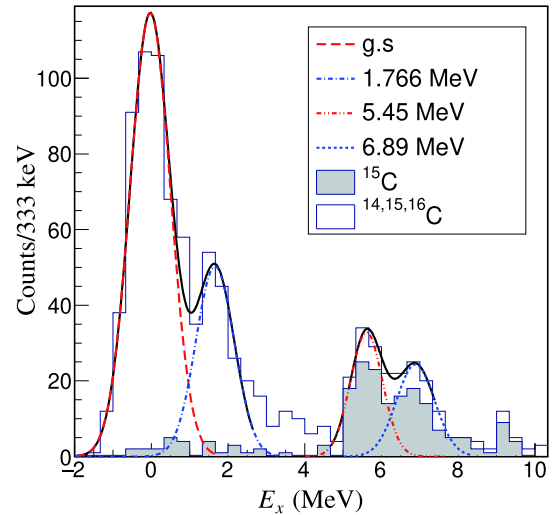


Fig. 2. (color online) Excitation energy spectra reconstructed from the energies and angles of the recoil deuterons in coincidence with $^{14,15,16}\text{C}$ (white histograms) or with ^{15}C (grey histograms).

ergies versus angles) spectrum of carbon isotopes according to the kinematics of $^{16}\text{C} + d$ inelastic scattering. Comparing to the spectra gated by all carbon isotopes (white histograms), the events at around the 6.89 MeV state reduce slightly, indicating that this state predominantly decays via $1n$ to the bound states in ^{15}C rather than via $2n$ to ^{14}C even though its excitation energy is higher than the $2n$ separation threshold ($S_{2n} = 5.468$ MeV). However, its specific decay path, namely to the g.s. or to the first excited state in ^{15}C , can not be determined just from the present experiment.

As shown in Fig. 3, four excitation energy spectra were constructed within an angular bin of 2° in the laboratory frame. The 5.45 MeV state is clearly measured in each spectrum. However, the 6.89 MeV resonance is hardly seen in Fig. 3 (d) because the recoil deuterons inelastically scattered from this state can not reach $66^\circ \sim 68^\circ$ according to the kinematics, as seen in Fig. 1. In Fig. 2 and Fig. 3, the events at around 3.5 MeV correspond to the mixture of the excited states at 3.03(0_2^+), 3.98(2^+), 4.088(3^+) and 4.142(4^+) MeV in ^{16}C . However, the statistics are too low to fix the excitation energy spectrum with so many states. Their effect on the differential cross sections of unbound states was estimated to be negligible.

The Gaussian and Breit–Wigner functions [25] were convoluted with the response function of the whole detection system to fit the bound and unbound states, respectively, in the excitation energy spectra (Figs. 2 and 3). The Breit–Wigner function with the energy-dependent width $\Gamma(E_r)$ is defined as [25]:

$$F(E_r) = \frac{\Gamma(E_r)}{(E_x - E_0)^2 + \Gamma^2(E_r)/4}, \quad (1)$$

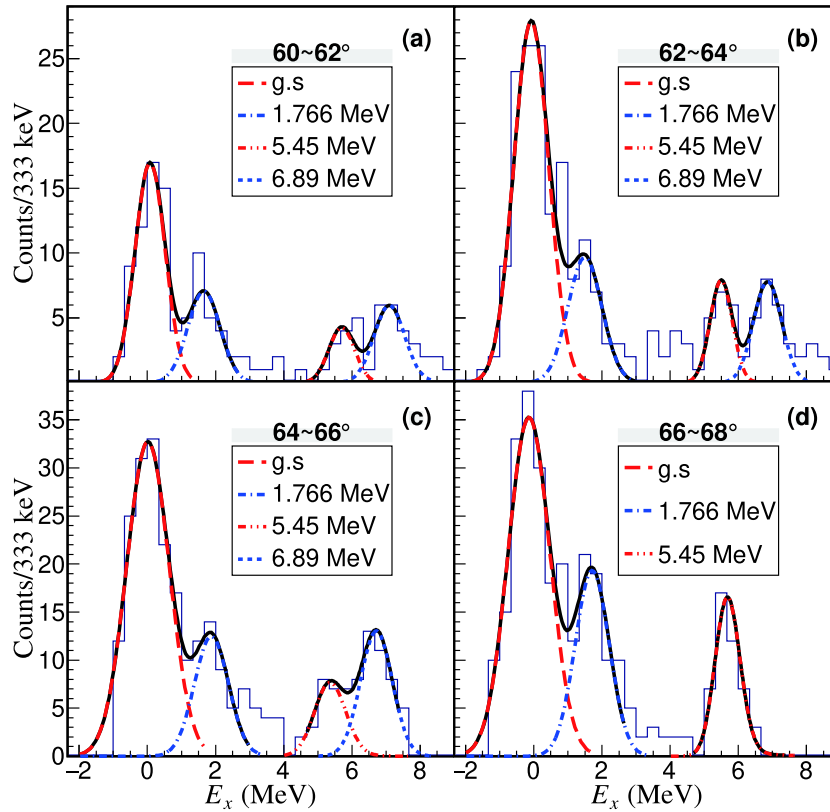


Fig. 3. (color online) With a gate of all carbon isotopes ($^{14,15,16}\text{C}$), excitation energy spectra deduced from the energies and angles of the recoil deuterons emitted at (a) $60^\circ\text{--}62^\circ$, (b) $62^\circ\text{--}64^\circ$, (c) $64^\circ\text{--}66^\circ$, and (d) $66^\circ\text{--}68^\circ$.

where E_r is the relative energy of the decay particles, E_0 and E_x are the centroid energy and the excitation energy of the resonant peak, respectively. The relationship between E_r and E_x is $E_x = E_r + S_n$, where $S_n = 4.25$ MeV is the $1n$ separation energy of ^{16}C [26]. Note that the 5.45 MeV state predominantly decays by $1n$ to the first excited state at $E_{1\text{st}} = 0.74$ MeV in ^{15}C rather than to its g.s. [19], therefore the equation $E_r = E_x - S_n - E_{1\text{st}}$ is used here. The energy-dependent width is defined as $\Gamma(E_r) \equiv g\sqrt{E_r}$, where g is a free parameter during the fitting procedure. We assumed that the 6.89 MeV state has the same decay path as the 5.45 MeV state, as they have the same excitation mode (see below). The response function was simulated using the GEANT4 package [27], taking into account the energy spread of the secondary beam (2.0%), the energy losses of the recoil deuterons in the CD_2 target, the energy and angular resolution of the actual experimental setup and so on [14]. The simulated resolutions for the 5.45 and 6.89 MeV states are 952 and 1050 keV (FWHM), respectively, which are not good enough to discriminate these two states from the 6.11 and 6.28 MeV states. By comparing the experimental excitation energy spectra to the simulation results with different mixture portion of the 6.11 and 6.28 MeV states, we found that the mixture of these two states is smaller than 20%. Therefore, we assumed that they are pure 5.45 and

6.89 MeV states in this paper. The intrinsic width of the 5.45 MeV resonance is deduced to be 3.5 keV ($g\sqrt{E_r}$), which is consistent with the conclusion from the $1n$ knockout reaction [19]. How should we understand such a narrow intrinsic $1n$ -decay width of the 5.45 MeV state? This near-threshold state is only 30 keV below the $2n$ emission threshold. Therefore, its wave function is coupled by the imprint of the $2n$ -decay channel, which leads to a very narrow decay width [28, 29]. The intrinsic width of the newly measured state is determined to be 10.2 keV.

The elastic scattering DCSs of $^{16}\text{C} + d$ have been published in Ref. [14]. The systematic optical potential (OP) parameters obtained from Daehnick *et al.* [30], An *et al.* [31], Han *et al.* [32], and Zhang *et al.* (DA1p) [33] were applied to describe the DCSs of $^{16}\text{C} + d$. In order to best fit the experimental data, the well depths of real (V_V) and imaginary parts ($W_V + W_S$) [4] were searched. The searching process were performed with the code SFRESCO [34] using the χ^2 minimization method. The best OP parameters are listed in Table 2.

The counts of the inelastically scattered deuterons were determined by fitting each Q -value spectrum displayed in Fig. 3. Comparing with the theoretical calculations, the DCSs for inelastic scattering to the two unbound states are plotted in Fig. 4. Only statistical errors

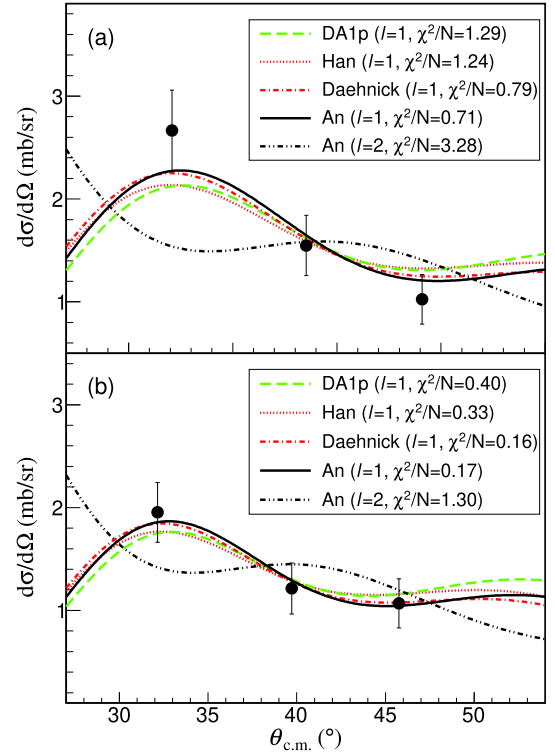
Table 2. Parameters of the optical model potentials extracted from the elastic scattering of $^{16}\text{C} + d$ [14]. The corresponding deformation lengths extracted from the inelastic scattering DCSs for the 5.45 and 6.89 MeV states are listed in the last two columns.

	V_0 /MeV	r_0 /fm	a_0 /fm	W /MeV	r_W /fm	a_W /fm	W_D /MeV	r_{W_D} /fm	a_{W_D} /fm	δ_d /fm 5.45 MeV	δ_d /fm 6.89 MeV
DA1p [33]	82.397	1.067	0.776	9.557	1.699	0.744	0.006	1.699	0.744	0.58	0.55
Daehnick <i>et al.</i> [30]	72.405	1.170	0.792	2.496	1.325	0.692	9.196	1.325	0.692	0.55	0.51
An <i>et al.</i> [31]	73.881	1.149	0.751	3.363	1.345	0.603	7.542	1.394	0.687	0.56	0.52
Han <i>et al.</i> [32]	74.017	1.174	0.809	6.787	1.563	0.813	6.346	1.328	0.578	0.56	0.53

are shown. The systematic errors are estimated to be about 10%, including the contributions from different cuts on the PID spectra to choose the recoil deuterons and carbon isotopes, the uncertainties in target thickness and in the simulation of solid angles. The background contribution from carbon in the CD_2 target was found to be negligible after analyzing the data from the carbon and the empty targets. It should be noted that the data points at 60° – 62° in the laboratory frame for the 5.45 MeV state were discarded for two reasons. First, the energies of deuterons are close to the threshold of the CsI(Tl) detector, leading to the loss of some events in this detector. Second, some recoil deuterons punch through the detectors sideways at the edges, resulting in incorrect measurement of their energies.

Distorted-wave Born approximation (DWBA) calculations were performed using the code FRESKO [34] in the framework of rotational model to extract the deformation length. The method is similar to that used in the inelastic scattering to the 2^+ state in ^{16}C [14]. Using the OP parameters obtained from the elastic scattering data and deformation length $\delta = 1.0$ as the starting points, the best δ values were searched using the code SFRESKO [34] with the minimum χ^2 method. With different OP parameters, different δ values are extracted and listed in Table 2. In Fig. 4, the black solid and the black dot-dashed curves stand for the DWBA calculations using the same systematic OP parameters obtained from An *et al.* [31] but with an $l = 1$ and an $l = 2$ excitation, respectively. It is clear that the $l = 1$ result gives a better reproduction of the experimental DSCs. In the rotational model, they assume an intrinsic shape that is common to the initial and final states. Thus, only the natural parity transitions with $(-1)^l$ (l is parity change) are allowed. In the case of an $l = 1$ transition, only the assumption of 1^- state is valid. For the 5.45 MeV state, the valid assumption of $J^\pi = 1^-$ is different from the spin-parity assignment of 2^- in Ref. [19], which needs more discussion (below) and studies to clarify.

The average δ values are 0.56 ± 0.05 (statistics) ± 0.06 (systematics) fm and 0.53 ± 0.05 (statistics) ± 0.05 (systematics) fm for the 5.45 and 6.89 MeV state, respectively. The statistical errors were obtained from the experimental DCSs, while the systematic errors were deduced from the results with different OPs used in the cal-

**Fig. 4.** (color online) Angular distributions of inelastic scatterings to the (a) 5.45 and (b) 6.89 MeV states in ^{16}C in comparison with the DWBA calculations using different OPs and the corresponding deformation lengths. See text for more details. Note that the DWBA calculations have been averaged over an angular range, which corresponds to the angular acceptance for each data point (2 degrees in the laboratory frame).

culations. The deformation lengths for the 5.45 and 6.89 MeV states (an $l = 1$ excitation) are consistent with each other within the error bar, but are different from that of 1.18 ± 0.15 for the 1.776 MeV state (an $l = 2$ excitation). This kind of difference was also found in ^{12}Be , where deformation lengths of 0.24 and 1.56 fm were extracted for the $E1$ and $E2$ cases, respectively [35]. This phenomenon demonstrates that ^{16}C has reduced deformation when being excited from the g.s. to the negative excited states, similar to the excitation of ^9Li [36]. The integrated cross sections are 6.42 and 5.41 mb for the 5.45 and 6.89 MeV states, respectively.

III. SHELL MODEL CALCULATIONS

For ^{16}C , shell model calculations were performed using the original and the modified YSOX interaction in the $3\hbar\omega$ model space [12, 37, 38]. Figure 5 plots the calculated results compared with the experimental data. The calculated results for the negative-parity states using the WBT interaction are also displayed [19]. The bound excited states are reasonably well reproduced by the calculations with the original model (YSOX1), but most of the calculated excitation energies are higher than the experimental data, especially for the unbound states above the $1n$ separation energy. The calculations with a decrease of 200 keV of $0d5/2$ -orbital (YSOX2) give a better description of the excited states. Note that such reduction in the YSOX interaction leads to a decrease of the $5/2^+$ state in ^{15}C and an increase of the $1/2^+$ and $5/2^+$ states in ^{17}C , but does not change the energy level sequence of the low-lying states in both ^{15}C and ^{17}C .

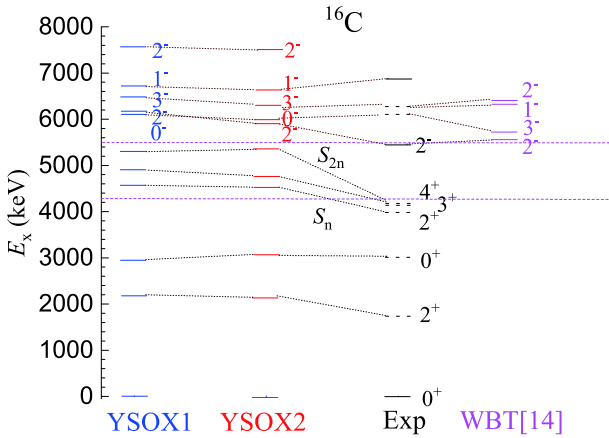


Fig. 5. (color online) Energy level scheme of ^{16}C compared with the shell model calculations using the original (YSOX1, blue) and modified (YSOX2, red) YSOX interaction [12], and the WBT interaction (WBT, purple) [19]. For the experimental results, the black solid and dotted lines stand for the states observed in the present and previous experiments, respectively.

The lowest two negative-parity states, 0^- and 2^- , are inverted if we use YSOX2 instead of YSOX1. Considering an $l = 1$ excitation for the 5.45 MeV state, both the spin-parities of 0^- and 2^- are possible. The configurations and neutron occupancies of the unbound negative-parity states with excitation energies lower than 8000 keV are listed in Table 3. Calculations from YSOX2 give a predominant $1\hbar\omega$ configuration for all these negative-parity states, demonstrating that the major excitation mode is the single-particle cross-shell excitation. The 0^- state has an obviously large s -shell neutron occupation

Table 3. Configurations and the neutron occupancies of the low-lying negative-parity states in ^{16}C , with YSOX2 in the $3\hbar\omega$ model space.

spin-parity	$1\hbar\omega$ (%)	$3\hbar\omega$ (%)	$N_{p1/2}$	$N_{p3/2}$	$N_{d3/2}$	$N_{d5/2}$	$N_{s1/2}$
2^-	92.4	7.6	1.169	3.279	0.260	2.147	0.635
0^-	92.7	7.3	1.185	3.772	0.173	1.925	0.945
3^-	92.2	7.8	1.178	3.784	0.264	2.009	0.765
1^-	92.8	7.2	1.291	3.666	0.195	2.091	0.757
2^-_2	92.4	7.6	1.225	3.737	0.223	1.778	1.037

number, while the 2^- state has a relatively large d -shell neutron occupation number. Thus, the assignment of 2^- is more appropriate than 0^- for the 5.45 MeV state because it decays predominantly to the first excited state of ^{15}C [19], in which state the valence neutron dominantly populates the d -orbital. This spin-parity assignment is consistent with Refs. [19, 22]. With more d -orbital components, 3^- and 1^-_2 are possible candidates for the 6.89 MeV state, which has the same decay path or the same excitation mode and excitation cross sections as the 5.45 MeV state [19]. The 2^-_2 state with more s -orbital neutrons is ruled out. Taking into account the DWBA calculation results, its spin-parity is most likely 1^-_2 . Note that, here, using the standard shell model instead of the continuum shell model for the description of resonances is not completely appropriate, thus the spin-parity assignment is very preliminary. The new tentative assignments are summarized in Table 1, where controversial spin-parity results for these negative-parity states are clearly seen. Thus, in the future, more experiments with better resolution are required to clarify these divergences.

IV. SUMMARY

In summary, two negative-parity states at $E_x = 5.45$, 6.89 MeV in ^{16}C were studied by deuteron inelastic scattering in inverse kinematics. The former is consistent with the previous experimental result from the $1n$ knockout from ^{17}C [19], while the latter resonance is newly observed in our experiment. The angular distributions of these two states were well reproduced by the DWBA calculations with an $l = 1$ excitation. The shell model calculations with the modified YSOX interaction in the $3\hbar\omega$ model space support the negative-parity assignment for these two states.

ACKNOWLEDGMENTS

We gratefully thank the IMP accelerator group for providing ^{18}O primary beam and the RIBLL collaboration for supplying a lot of electronics.

References

- [1] W. Liu, J. L. Lou, Y. L. Ye *et al.*, *Nucl. Sci. Tech.* **31**, 20 (2020)
- [2] G. Li, Z. W. Tan, J. L. Lou *et al.*, *Nucl. Phys. Rev.* **37**, 3 (2020)
- [3] Y. Jiang, J. L. Lou, Y. L. Ye *et al.*, *Chin. Phys. Lett.* **35**(8), 082501 (2018)
- [4] J. Chen, J. L. Lou, Y. L. Ye *et al.*, *Phys. Rev. C* **93**, 034623 (2016)
- [5] J. Chen, J. L. Lou, Y. L. Ye *et al.*, *Phys. Rev. C* **94**, 064620 (2016)
- [6] J. Chen, J. L. Lou, Y. L. Ye *et al.*, *Phys. Lett. B* **781**, 412 (2018)
- [7] J. Chen, J. L. Lou, Y. L. Ye *et al.*, *Phys. Rev. C* **98**, 014616 (2018)
- [8] J. Chen, S. M. Wang, H. T. Fortune *et al.*, *Phys. Rev. C* **103**, L031302 (2021)
- [9] W. Liu, J. L. Lou, Y. L. Ye *et al.*, *Phys. Rev. C* **104**, 064605 (2021)
- [10] X. Pereira-López, B. Fernández-Domínguez, F. Delaunay *et al.*, *Phys. Lett. B* **811**, 135939 (2020)
- [11] M. Stanoiu, D. Sohler, O. Sorlin *et al.*, *Phys. Rev. C* **78**, 034315 (2008)
- [12] C. X. Yuan, T. Suzuki, T. Otsuka *et al.*, *Phys. Rev. C* **85**, 064324 (2012)
- [13] V. Maddalena, T. Aumann, D. Bazin *et al.*, *Phys. Rev. C* **63**, 024613 (2001)
- [14] Y. Jiang, J. L. Lou, Y. L. Ye *et al.*, *Phys. Rev. C* **101**, 024601 (2020)
- [15] Y. Liu, Y. L. Ye, J. L. Lou *et al.*, *Phys. Rev. Lett.* **124**, 192501 (2020)
- [16] J. X. Han, Y. Liu, Y. L. Ye *et al.*, *Phys. Rev. C*, in review
- [17] H. T. Fortune, R. Middleton, M. E. Cobern *et al.*, *Phys. Lett. B* **70**, 408 (1977)
- [18] R. R. Sercely, R. J. Peterson, and E. R. Flynn., *Phys. Rev. C* **17**, 1919 (1978)
- [19] Y. Satou, J. W. Hwang, S. Kim *et al.*, *Phys. Lett. B* **728**, 462-466 (2014)
- [20] L. C. Tao, Y. Ichikawa, C. X. Yuan *et al.*, *Chin. Phys. Lett.* **36**, 062101 (2019)
- [21] H. T. Fortune, M. E. Cobern, S. Mordechai *et al.*, *Phys. Rev. Lett.* **40**, 1236 (1978)
- [22] H. T. Fortune and Y. Satou, *Phys. Rev. C* **90**, 034308 (2014)
- [23] H. T. Fortune, *Phys. Rev. C* **94**, 014305 (2016)
- [24] H. J. Ong, N. Imai, D. Suzuki *et al.*, *Phys. Rev. C* **78**, 014308 (2008)
- [25] J. Tanaka, R. Kanungod, M. Alcorta *et al.*, *Phys. Lett. B* **774**, 268-272 (2017)
- [26] M. Wang, G. Audi, A. H. Wapstra *et al.*, *Chin. Phys. C* **36**, 1603 (2012)
- [27] S. Agostinelli, J. Allison, and K. Amako, *Nucl. Instrum. Methods Phys. Res., Sect. A* **506**, 250 (2003)
- [28] J. Okolowicz, M. Ploszajczak, and W. Nazarewicz, *Prog. Theor. Phys. Supplement* **196**, 230 (2012)
- [29] J. Okolowicz, W. Nazarewicz, and M. Ploszajczak, *Fortschr. Phys.* **61**, 66-79 (2013)
- [30] W. W. Daehnick, J. D. Childs, and Z. Vrcelj, *Phys. Rev. C* **21**, 2253 (1980)
- [31] H. X. An and C. H. Cai, *Phys. Rev. C* **73**, 054605 (2006)
- [32] Y. L. Han, Y. Y. Shi, and Q. B. Shen, *Phys. Rev. C* **74**, 044615 (2006)
- [33] Y. Zhang, D. Y. Pang, and J. L. Lou, *Phys. Rev. C* **94**, 014619 (2016)
- [34] I. J. Thompson, *Comput. Phys. Rep* **7**, 167 (1988)
- [35] H. Iwasaki, T. Motobayashi, H. Akiyoshi *et al.*, *Phys. Lett. B* **491**, 8-14 (2000)
- [36] H. Al Falou, R. Kanungo, C. Andreoiu *et al.*, *Phys. Lett. B* **721**, 224-228 (2013)
- [37] C. X. Yuan, C. Qi, and F. R. Xu, *Nucl. Phys. A* **883**, 25-34 (2012)
- [38] C. X. Yuan, *Chin. Phys. C* **41**, 104102 (2017)